

On the peculiarities of the magnetic polaron hole spectrum in high- T_c superconductors

A.F. Barabanov

Vereshagin Institute for High Pressure Physics, 142092 Troitsk, Moscow Region, Russian Federation

L.A. Maksimov and L.E. Zhukov

Kurchatov Institute, 123182 Moscow, Russian Federation

Received 19 July 1993; accepted for publication 27 August 1993

Communicated by V.M. Agranovich

The one hole spectrum $\epsilon(\mathbf{k})$ in the CuO_2 plane is studied in the framework of the magnetic polaron approach on the basis of the two-band Hubbard model. The manifested strong temperature dependence of the spectrum $\epsilon(\mathbf{k})$ is connected with the temperature behavior of the spin correlation functions. It is also shown that for an accurate description of the lowest band bottom position it is important to take into account the dependence of the hopping amplitude on the hopping trajectory and to extend the simplest Zhang-Rice site basis.

1. Introduction

Up to date much theoretical work has been performed in order to study the spectrum of electrons whose motion depends on the localized spin state. The case of the two band strong coupling model is an example of such a system [1]. As it is known, this model is used for the explanation of the properties of CuO_2 planes in high- T_c superconductors (HTSC). The hole Hamiltonian of this model is [2]

$$\hat{H} = \hat{T} + J \sum_{\langle R, R' \rangle} S_R S_{R'}, \quad (1)$$

$$\begin{aligned} \hat{T} = & \sum_{\substack{R, a_1, a_2 \\ \sigma_1, \sigma_2}} [\tau(1 - \delta_{a_1, a_2} \delta_{\sigma_1, \sigma_2})] \\ & \times Z_R^{\sigma_1 \sigma_2} C_{R+a_2, \sigma_2}^+ C_{R+a_1, \sigma_1}, \\ & a_1, a_2 = \pm a_x, \pm a_y, \quad \tau = t^2 / \epsilon_{pd}. \end{aligned} \quad (2)$$

Here and below $r = R + a$ are the four vectors of the O sites nearest to the Cu site R (see fig. 1); the operator C_σ^+ creates a hole with a spin index $\sigma = \pm 1$ at the O site and $Z_R^{\sigma_1 \sigma_2}$ is the Hubbard projection operator which is introduced to exclude the doubly oc-

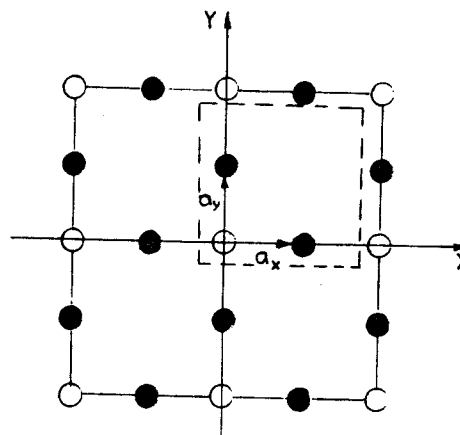


Fig. 1. The structure of the CuO_2 plane: (O) Cu sites, (●) O sites, a_x and a_y are the O-site vectors in the unit cell.

cupied states of the Cu sites and describe spin flip on them.

The first term \hat{T} in (1) describes the effective hole hopping from O to O sites through the intervening Cu sites. It can be obtained within the perturbation theory in $t/\epsilon_{pd} \ll 1$ from the site Hamiltonian which is characterized by the Cu and O hole levels ϵ_d and ϵ_p ($\epsilon_{pd} = \epsilon_p - \epsilon_d > 0$), by the NN Cu-O hopping t , and by the intrasite Hubbard repulsion energies U_d and

U_p , respectively. We put $U_d = \infty$ as the largest energy parameter and consider the case $U_p = 0$.

The second term in Hamiltonian (1) describes the antiferromagnetic (AFM) exchange interaction $J > 0$ between nearest copper sites with spins $S = \frac{1}{2}$.

It is known, that in the case of Hamiltonian (1) the hole wave function should be described in the framework of the magnetic polaron approach [3]. The role of exchange interaction is to stabilize the size of the polaron and if $J > 0.2\tau$, then one can consider only the small radius polaron [4]. Thus, fixing the size of the polaron it is possible to describe the polaron motion only through the hopping Hamiltonian \hat{T} (2).

In this paper we study the spectrum ϵ_k of a small radius magnetic polaron on the background of a strongly correlated magnetic subsystem state $|G\rangle$. It is assumed that $|G\rangle$ is the RVB type singlet state with zero average spin on each site and spherically symmetric spin correlation functions [5].

Section 2 of this paper is devoted to the study of the temperature dependence of the hole spectrum. The spectrum should essentially depend on the spin correlation functions and as they change with temperature increase, one obtains the temperature dependence of the polaron spectrum. In this section we also consider the importance of the extension of the basis functions for a correct ϵ_k description.

In section 3 we study the fine structure of the ϵ_k spectrum which arises from additional real details of the accepted model. In particular, we take into account the dependence of the hole hopping amplitude on the hopping trajectory.

The conclusion contains a brief summary of results.

2. Temperature dependence of the magnetic polaron spectrum

In this section we study the dependence of ϵ_k on the temperature behavior of the spin correlation functions.

The simplest approach to the magnetic polaron description uses the site wave function, which is analogous to the Zhang-Rice polaron [3],

$$\varphi_R = \frac{1}{2} \sum_{\mathbf{a} = \pm \mathbf{a}_x, \pm \mathbf{a}_y} (C_{\mathbf{R}+\mathbf{a},+1} Z_{\mathbf{R}}^- - C_{\mathbf{R}+\mathbf{a},-1} Z_{\mathbf{R}}^+) |G\rangle. \quad (3)$$

Having chosen the ground state and using the variation method one can obtain the following expression for the ϵ_k spectrum,

$$\epsilon_k = \langle \varphi_k | \tau | \varphi_k \rangle / \langle \varphi_k | \varphi_k \rangle,$$

$$\varphi_k = \sum_{\mathbf{R}} e^{i\mathbf{k}\cdot\mathbf{R}} \varphi_{\mathbf{R}}, \quad \langle \rangle \equiv \langle G | \langle G \rangle,$$

$$\epsilon_k = -4\tau + \frac{\tau}{1+A\gamma_k} [-4A\gamma_k + B(\gamma_k^2 - \frac{1}{4}) + (C_{x+y} - C_{2x}) \cos(2k_x a) \cos(2k_y a)], \quad (4)$$

where

$$\gamma_k = \frac{1}{2} [\cos(2k_x a) + \cos(2k_y a)]. \quad (5)$$

As can be seen from (5) the expression of the ϵ_k spectrum explicitly contains the spin correlation functions (6) between the first, second and third nearest neighbors,

$$A = \frac{1}{4} + C_1, \quad B = 4(\frac{1}{8} + \frac{1}{2}C_{2x} - C_1), \\ C_1 = \langle \mathbf{S}_n \cdot \mathbf{S}_{n+2\mathbf{a}_i} \rangle, \quad C_{i+j} = \langle \mathbf{S}_n \cdot \mathbf{S}_{n+2\mathbf{a}_j+2\mathbf{a}_i} \rangle, \\ \mathbf{a}_i \neq -\mathbf{a}_j, \quad \mathbf{a}_i, \mathbf{a}_j = \pm \mathbf{a}_x, \pm \mathbf{a}_y. \quad (6)$$

In this section we use the simplest approach and put $C_{2x} = C_{x+y} = C_2$ [6]. In this case the ϵ_k spectrum depends only on γ_k [4],

$$\epsilon_k = -4\tau + \frac{\tau}{1+A\gamma_k} [-4A\gamma_k + B(\gamma_k^2 - \frac{1}{4})]. \quad (7)$$

The spin correlation functions of the CuO_2 plane are usually described in the framework of the $S = \frac{1}{2}$ AFM two-dimensional Heisenberg model on the square lattice [7]. At low temperatures the spin correlation functions have an AFM character and strive for their paramagnetic limit with temperature increase [8]. For an accurate utilization of these properties we chose the RVB type spherical symmetric $|G\rangle$ state as the ground state. The numerical values of the coefficients C_1 and C_2 at zero temperature can be calculated by different methods and their behavior in a wide range of temperatures was obtained in ref. [9], which results we will use. The typical values

$C_1 = -0.35$ and $C_2 = 0.22$ indicate strong AFM correlations in the copper subsystem at low temperatures. This results in a small value of the γ_k term in (7) compared with the γ_k^2 term, as $|A| \approx 0.1 \ll B \approx 2.33$. The coefficient A of the linear term is proportional to the amplitude of hopping between different copper sublattices and the coefficient B is proportional to hopping in the same copper sublattice, though in reality there are no sublattices in the spherical symmetric $|G\rangle$ state. Thus, due to the magnetic correlations, the polaron mainly moves along one of the sublattices. Let us mention, that in the case of a $|G\rangle$ state with two sublattices (Néel type) the spectrum ϵ_k would contain only even degrees γ_k^{2n} . This would lead to the symmetric location of equienergy lines relative to the magnetic Brillouin zone boundary. The RVB type ground state eliminates this degeneracy.

The bottom of the ϵ_k spectrum band coincides with the line $\gamma_k = \text{const}$. For the above values of the coefficients C_1 and C_2 (low temperatures) the ϵ_k spectrum minimum is represented in fig. 2 by line 1. This line is located near the magnetic Brillouin zone boundary and is defined by the equation $\gamma_k = -0.071$. For the typical doping value $x = 0.2$ for $\text{La}_{2-x}\text{Sr}_x\text{CuO}_4$ one of the Fermi surface sheets is located close to the Van Hove points X – the corners of the magnetic

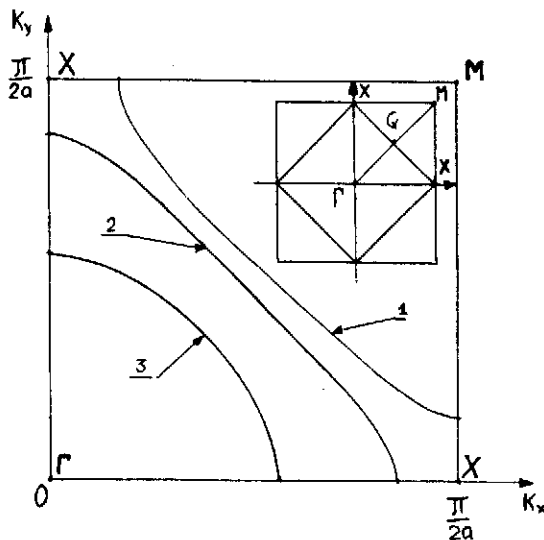


Fig. 2. The position of the ϵ_k (5) band bottom in the first quadrant of the Brillouin zone at different temperatures is shown by the lines: (1) $T/J=0$ ($C_1 = -0.35$, $C_2 = 0.22$); (2) $T/J=1$ ($C_1 = -0.22$, $C_2 = 0.09$) and (3) $T/J=\infty$ ($C_1 = 0$, $C_2 = 0$). The complete and magnetic Brillouin zones are shown in the inset.

Brillouin zone. Then the density of states has singularities near the bottom of the band and near these Van Hove points. This circumstance gives the foundation for superconductivity in a 2D system with nesting and nonmonotonic T_c behavior on doping and applying pressure [10].

In fig. 2 lines 2 and 3 represent the location of the ϵ_k band bottom for the correlation functions $C_1 = -0.22$, $C_2 = 0.09$ and $C_1 = 0$, which have the temperatures $T/J = 1$ and $T/J = \infty$ [9]. It can be seen that the temperature increase leads to the shift of the band bottom lines to point Γ . Then it turns out that the equienergy lines corresponding to the Fermi surface with fixed hole hopping, change their curvature. With temperature increase the Fermi surface lines have the tendency to cross the magnetic Brillouin zone boundary and move away from the Van Hove points. In particular the Fermi surface at high temperatures $T \gg J$ coincides with two lines close to a circumference with the center in the point Γ .

Let us consider the simplest extension of the basis of trial functions from the Zhang–Rice (3) polaron up to the six following functions,

$$\begin{aligned} \varphi_R^1 &= (C_{R+a_x, +1}^+ Z_{R-}^- - C_{R+a_x, -1}^+ Z_{R-}^+) |G\rangle, \\ \varphi_R^2 &= (C_{R+a_y, +1}^+ Z_{R-}^- - C_{R+a_y, -1}^+ Z_{R-}^+) |G\rangle, \\ \varphi_R^3 &= (C_{R+a_x, +1}^+ Z_{R+2a_x}^- - C_{R+a_x, -1}^+ Z_{R+2a_x}^+) |G\rangle, \\ \varphi_R^4 &= (C_{R+a_y, +1}^+ Z_{R+2a_y}^- - C_{R+a_y, -1}^+ Z_{R+2a_y}^+) |G\rangle, \\ \varphi_R^5 &= C_{R+a_x, +1}^+ |G\rangle, \quad \varphi_R^6 = C_{R+a_y, +1}^+ |G\rangle. \end{aligned} \quad (8)$$

The set of functions (8) preserves the small radius of the polaron and describes the state of the system with the whole spin and its projection equal to $\frac{1}{2}$.

In the same way as above the hole spectrum $\tilde{\epsilon}_k$ can be obtained by transformation to the momentum representation and by solving the appropriate secular 6×6 equation for Hamiltonian \hat{T} (2). We are interested in the behavior of the lowest band, which is analogous to the behavior of the spectrum ϵ_k (7). It appears, that in the limit case $T=0$ the spectra $\tilde{\epsilon}_k$ and ϵ_k are indistinguishable.

But in the paramagnetic limit ($C_1 = C_2 = 0$) the spectrum $\tilde{\epsilon}_k$ qualitatively differs from the spectrum ϵ_k . The spectra ϵ_k and $\tilde{\epsilon}_k$ are both shown in fig. 3 in the direction ΓM . As is seen the bottom of the spectrum $\tilde{\epsilon}_k$ is degenerated in the point Γ , that is the center of the Brillouin zone. This means that under small doping the Fermi surface consists of one line (not

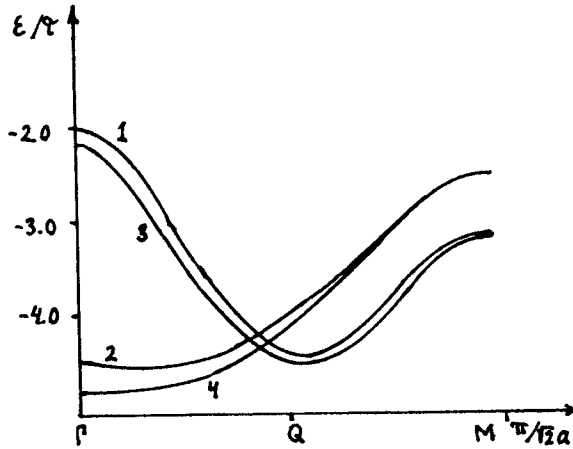


Fig. 3. The spectra ϵ_k (7) and $\tilde{\epsilon}_k$ are shown in the ΓM direction. Lines (1) and (2) correspond to the spectrum ϵ_k in the cases $T/J=0$ and $T/J=\infty$ and the lines (3) and (4) accordingly to the spectrum $\tilde{\epsilon}_k$.

two as in the ϵ_k case) close to the circumference.

Thus, at low temperatures the Zhang–Rice polaron (3) correctly describes the behavior of the lowest band of the ϵ_k spectrum, but in the paramagnetic limit one should use the extended basis of wave functions (8).

3. Influence of the model details on the spectrum ϵ_k

In this section we study the influence of realistic model details on the magnetic polaron spectrum. We will restrict our consideration to the “low temperature” range $T \leq 0.3J \sim 300$ K (the typical value of the intraplane AFM exchange parameter J for HTSC is about 1000 K). As mentioned in section 1 Hamiltonian (2) takes into account the first term in the p–d hybridization parameter t . Consideration of the higher order terms in the t/ϵ_{pd} expansion must lead to the dependence of the hopping amplitude on hopping trajectories. This means that in Hamiltonian (2) the amplitude of hole hopping between the oxygen sites $R+a_x$ and $R+a_y$ (τ_{x+y}) should differ from the amplitude of hole hopping between $R-a_x$ and $R+a_x$ (τ_{2x}) sites. The same effect must occur if we allow for d–p hybridization between distinct Cu–O site orbitals or direct O–O hopping. Then the hopping Hamiltonian should be

$$\hat{T} = \sum_{\substack{R, a_1, a_2 \\ \sigma_1, \sigma_2}} (\tau_{2x} \delta_{a_1, -a_2} + \tau_{x+y} \delta_{a_1 \perp a_2} + \tau_0 \delta_{a_1, a_2} \delta_{\sigma_1, -\sigma_2}) Z_R^{\sigma_1 \sigma_2} C_{R+a_2, \sigma_2}^+ C_{R+a_1, \sigma_1}, \quad (9)$$

where τ_0 is the amplitude of hole spin variation in one site. We denote $\tau_{2x} = \tau_2$ and $\tau_{x+y} = \tau_2 + \delta\tau$. The behavior of the spectrum near the bottom of the band weakly depends on τ_0 and below we put $\tau_0 = \tau_2$. As it was mentioned before, in the case of low temperatures we can restrict the analysis to the minimal set of trial functions – the Zhang–Rice polaron. Then we obtain the spectrum ϵ'_k ,

$$\epsilon'_k = \epsilon_k + 2\delta\tau \{ -1 + [-A\gamma_k + B/4 \cos(2k_x a) \cos(2k_y a)] / (1 + A\gamma_k) \}. \quad (10)$$

This spectrum has a more complex dependence on (k_x, k_y) than ϵ_k (7). The equienergy lines for ϵ'_k are shown in fig. 4 for two different cases: (a) $\delta\tau < 0$ and (b) $\delta\tau > 0$.

As it can be seen from fig. 4 in case (a) there is a minimum near the equivalent points Q (points N). Then for small doping the Fermi surface must have a hole character ($R_H > 0$). If the concentration of holes increases, the Fermi surface transforms into two lines, qualitatively close to those of the spectrum ϵ_k . The variation of the curvature of the lines should lead to the decrease of R_H observed in the experiments [11]. The calculation of the effective hopping amplitude in the framework of the singlet-triplet model actually leads to the estimates $\tau_{x+y} < \tau_{2x}$ [12]. Let us emphasize that the whole amplitude of the hole hopping from the $R+a_x$ to the $R+a_y$ site is $2\tau_{2x}$, as there are “two ways” of hopping over two different copper sites.

The analogous position of the minimum near the Q point was obtained in the framework of Hamiltonian (2) taking into account direct O–O hopping between nearest O-neighbors [4]. Concrete consideration of p–p orbital hybridization in the CuO_2 system leads to such a sign of the direct O–O hopping term which decreases effective the amplitude τ_{x+y} in comparison with τ_{2x} .

We can also mention the well-known correspondence between the spectrum in fig. 4a and the spectra of the t – J and t – J – J models [13].

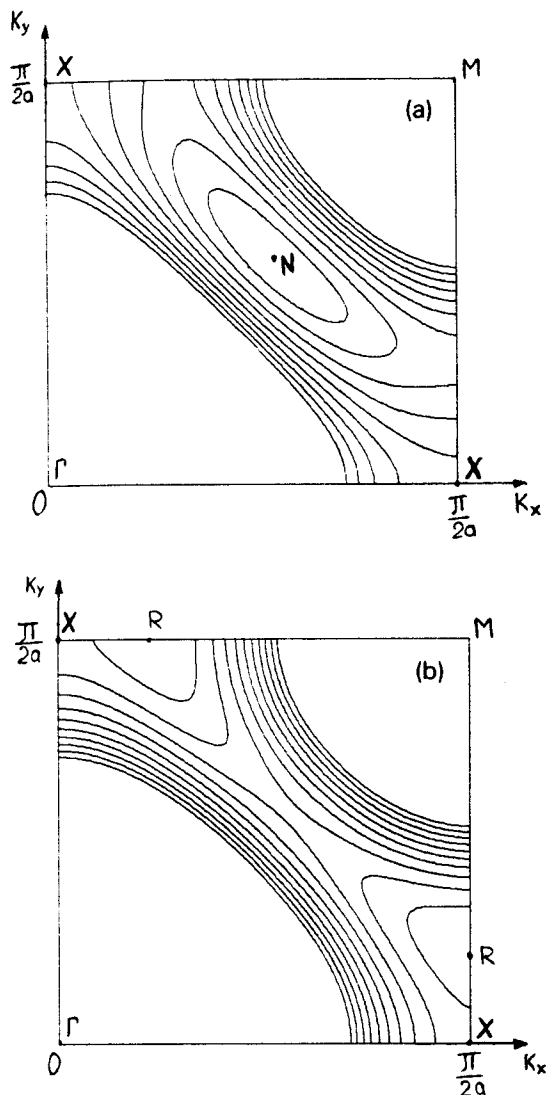


Fig. 4. The equienergy lines with the intervals $\Delta\epsilon/\tau_{2x}=0.04$ and the position of the band bottom for the spectrum ϵ_k (10) are shown for (a) $\tau_{x+y}/\tau_{2x}=0.7$ and (b) $\tau_{x+y}/\tau_{2x}=1.3$.

As can be seen from fig. 4b in the case $\delta\tau > 0$ the spectrum has four minima in the equivalent points R on the Brillouin zone boundary.

In our previous discussion we assumed $C_{x+y}=C_{2x}$. In reality, calculations of these correlation functions in the spherical symmetric model at $T=0$ lead to the values $C_{x+y}=0.23 > C_{2x}=0.20$ [9]. This circumstance in the framework of Hamiltonian (2) leads to a spectrum qualitatively analogous to spectrum (10) in the case $\delta\tau > 0$ (fig. 4b).

Thus, there are two main factors in this model which proceed from different tendencies: the difference of the hopping amplitude $\tau_{x+y} < \tau_{2x}$ promotes

formation of minima in points like N and the difference between correlation functions – in points like R. In reality, the factor which leads to the formation of minima in points of type N should predominate if we take into account finite hole concentration.

As is known finite hole concentration actually leads to frustrations in the spin subsystem [14]. Then, the existence of frustrations leads to an essential decrease of the correlation function C_{x+y} in comparison with C_{2x} . The calculation within the framework of the spherical symmetric model with the frustration parameter $\alpha=J_1/J_2 \approx 0$ (J_1 and J_2 are the AFM exchange interaction between NN and NNN Cu sites) gives $C_{x+y}=C_{2x}$ [15]. So the factor which leads to the shift of the minimum to point R disappears. So in the real situation of finite doping one can expect the existence of a minimum in the N type points.

4. Conclusion

In conclusion let us formulate the basic results obtained for the small radius magnetic polaron spectrum.

The temperature behavior of the spin subsystem correlation functions can essentially change the hole spectrum. The bottom of the lower band at low temperatures lies close to the magnetic Brillouin zone boundary and, then, near the points X which are responsible for the Van Hove singularities. In the high temperature limit the bottom of the band coincides with the center of the Brillouin zone. The Fermi surface curvature changes with temperature. In order to describe properly the spectrum in the paramagnetic limit one should use an extended basis of site functions, but not the simplest Zhang–Rice approach.

In the low temperature interval it is very important to take into account the dependence of the hole hopping amplitude on its trajectory. This circumstance leads to the formation of a local minimum near the Q point $k=(\pi/4a)(\pm 1, \pm 1)$. So, our consideration shows that the detailed elaboration of the initial Hamiltonian is very important for the accurate description of the lowest band of the magnetic polaron spectrum on the CuO_2 plane.

References

- [1] V.J. Emery, Phys. Rev. Lett. 58 (1987) 2794;
C.M. Varma, S. Schmitt-Rink and E. Abrahams, Solid State Commun. 62 (1987) 681.
- [2] V.J. Emery and G. Reiter, Phys. Rev. B 39 (1988) 4547.
- [3] R.C. Zhang and T.M. Rice, Phys. Rev. Lett. B 37 (1988) 3759;
A.F. Barabanov, L.A. Maksimov and G.V. Uimin, JETP Lett. 47 (1988) 622; Zh. Eksp. Teor. Fiz. 96 (1988) 655.
- [4] A.F. Barabanov, R. Kuzian and L.A. Maksimov, Supercond. Phys. Chem. Technol. 3 (1990) 8; J. Phys. Condens. Matter 3 (1991) 9129.
- [5] D.P. Arovas and A. Auerbach, Phys. Rev. B 38 (1988) 316;
A.F. Barabanov, L.A. Maksimov and O.A. Starykh, Int. J. Mod. Phys. B 4 (1990) 2319.
- [6] S. Liang, B. Doucot and P.W. Anderson, Phys. Rev. Lett. 61 (1988) 365.
- [7] J.M. Tranquada et al., Phys. Rev. B 38 (1988) 2477.
- [8] R.J. Birgenau et al., Phys. Rev. B 38 (1988) 6614;
Y. Endoh et al., Phys. Rev. B 37 (1988) 7443.
- [9] H. Shimahara and S. Takada, J. Phys. Soc. Japan 60 (1991) 2394.
- [10] Yu.V. Kopaev, JETP Lett. 47 (1988) 628;
A.N. Kozlov, L.A. Maksimov and A.F. Barabanov, Physica C 200 (1992) 183;
A.F. Barabanov, L.A. Maksimov and L.E. Zhukov, Physica C, in press.
- [11] T. Takagi et al., Phys. Rev. B 40 (1989) 2254.
- [12] S.V. Lovtsov and V.Yu. Yushankai, Physica C 179 (1991) 159.
- [13] C.X. Chen, M.B. Schuttler and A.J. Fedro, Phys. Rev. B 41 (1990) 2581;
C. Poiblan and E. Dagotto, Phys. Rev. B 42 (1990) 4861.
- [14] M. Inui, S. Doniach and M. Gabay, Phys. Rev. B 38 (1988) 6631.
- [15] A.F. Barabanov and V.M. Berestovsky, to be published.